Trapping a C_2 Radical in Endohedral Metallofullerenes: Synthesis and Structures of $(Y_2C_2)@C_{82}$ (Isomers I, II, and III)

Takashi Inoue,[†] Tetsuo Tomiyama,[†] Toshiki Sugai,[†] Toshiya Okazaki,[†] Takako Suematsu,[‡] Naoyuki Fujii,[‡] Hiroaki Utsumi,[‡] Kazutetsu Nojima,[‡] and Hisanori Shinohara*[,†,§]

Department of Chemistry and Institute for Advanced Research, Nagoya University, Nagoya 464-8602, Japan, JEOL Ltd., Akishima, Tokyo 196-8558, Japan, and CREST, JST

Received: January 11, 2004

Three isomers of yttrium carbide (Y_2C_2) endohedral metallofullerenes, i.e., $(Y_2C_2)@C_{82}$(I, II, III), have been synthesized and chromatographically isolated for the first time. The structures of $(Y_2C_2)@C_{82}$(I, II, III) metallofullerenes have been characterized by ^{13}C NMR measurements, whose molecular symmetries have been determined to be C_s, C_{2v}, and C_{3v}, respectively. In addition, a pure diyttrium metallofullerene, $Y_2@C_{82}$(III), has also been synthesized and structurally characterized. The ^{13}C NMR structural analyses indicate that $(Y_2C_2)@C_{82}$(III) has exactly the same fullerene cage as that of $Y_2@C_{82}$(III). On the basis of the results, we propose a C_2-trapping and loss of growth mechanism of dimetallofullerenes of $(M_2C_2)@C_{82}$ and $M_2@C_{82}$ from $M_2@C_{84}$, respectively.

Introduction

Fullerenes containing metal atom(s) inside the cage, the so-called endohedral metallofullerenes, have been successfully produced, extracted/isolated, and structurally characterized during the past decade.[1] The novel structures of various metallofullerenes have been investigated by X-ray diffraction[2−13] and ^{13}C NMR.[14−22] Recently, endohedral cluster metallofullerenes, where metal clusters,[5,8] metal nitride clusters,[10,11,13] and metal-carbide clusters[7,22] are encapsulated in the hollow space of fullerenes, have been recognized as a new type of endohedral metallofullerenes. In particular, metal-carbide endohedral fullerenes have been known as one of the cluster endohedral fullerenes encapsulating a metal-carbide cluster M_2C_2 (M = Sc, Y).[7,22]

A scandium-carbide metallofullerene, $(Sc_2C_2)@C_{84}$, has been known as the first metal-carbide endohedral metallofullerene reported by the present group.[7] The $(Sc_2C_2)@C_{84}$ endohedral structure with a Sc_2C_2 carbide cluster inside was clearly determined by ^{13}C NMR and powder X-ray diffraction measurements. More recently, the second example of a metal-carbide endohedral metallofullerene, $(Y_2C_2)@C_{82}$, was confirmed by ^{13}C NMR measurements.[22] The Sc_2C_2 and Y_2C_2 clusters within the carbon cages have been found to rotate around the molecular axes of the fullerenes.

Monoyttrium metallofullerene $Y@C_{82}$ is one of the first metallofullerenes extracted from arc-processed soot and characterized by electron paramagnetic resonance (EPR).[23,24] Furthermore, $Y@C_{82}$(isomer I) is the first metallofullerene in which the endohedral nature of the metal atom was confirmed, for the first time, by synchrotron X-ray powder diffraction.[2] On the other hand, dimetallofullerenes with two metal atoms encapsulated inside normally show diamagnetic property, which can allow us to determine their cage symmetry and endohedral structure by high-resolution ^{13}C NMR measurements.[14−16,19,22] Although $M_2@C_{80}$,[9,16] $M_2@C_{82}$,[12,25−31] and $M_2@C_{84}$[3,14,15,25,29] (where M is metal atom) have been known as abundantly obtained dimetallofullerenes, nobody so far could explain why metal atoms tend to be encapsulated in these specific cages of C_{80}, C_{82}, and C_{84} and why they are magic fullerene cages for the dimetallofullerenes.

Here, we report that all three isomers of Y_2C_{84} currently synthesized are metal-carbide endohedral fullerenes, i.e., $(Y_2C_2)@C_{82}$ (isomer I, II, III). The cage symmetries of $(Y_2C_2)@C_{82}$(I, II, III) were determined, respectively, to be C_s, C_{2v}, and C_{3v} by ^{13}C NMR measurements. The cage structures of $(Y_2C_2)@C_{82}$(II, III) were specified to be C_{82}-C_{2v}(9) and C_{82}-C_{3v}(8), respectively.

Furthermore, the absorption spectrum of $(Y_2C_2)@C_{82}$(III)[22] is almost exactly the same as that of the conventional pure diyttrium metallofullerene, $Y_2@C_{82}$(III), and the two metallofullerenes have been found to possess C_{82}-C_{3v}(8) cage symmetry. The only structural difference between $(Y_2C_2)@C_{82}$(III) and $Y_2@C_{82}$(III) is the presence and nonpresence of C_2 species in the cage, respectively.

On the basis of the present study, it is predicted that the cages of $M_2@C_{82}$(I, II, III) (M = Er and Tm)[12,25−27,30,31] might be the same as those of metal-carbide endohedral fullerenes $(Y_2C_2)@C_{82}$(I, II, III), respectively. These three C_{82} isomers possess cage structures similar to that of the C_{80}-I_h cage. The present study can provide us an important clue on the growth mechanism of the dimetallofullerenes $M_2@C_{82}$ and $(M_2C_2)@C_{82}$.

Experimental Section

Yttrium metallofullerenes were produced by the DC arc-discharge method.[1,22] The soot containing yttrium metallofullerenes was collected anaerobically and extracted with *o*-xylene solvent. The yttrium metallofullerenes $(Y_2C_2)@C_{82}$(I, II, III) and $Y_2@C_{82}$(I, II, III) were separated and isolated from various empty fullerenes and other yttrium metallofullerenes by the multistage high-performance liquid chromatography (HPLC) method[22,28,29] with four different types of columns [5PYE (20 mm diameter × 250 mm, Nacalai Tesque, 15 mL/min flow rate), Buckyclutcher I (21.1 mm diameter × 500 mm, Regis Chemical, 10 mL/min flow rate), 5PBB (20 mm diameter

[†] Nagoya University.
[‡] JEOL Ltd.
[§] CREST, JST.

10.1021/jp049865f CCC: $27.50
Published on Web 05/07/2004

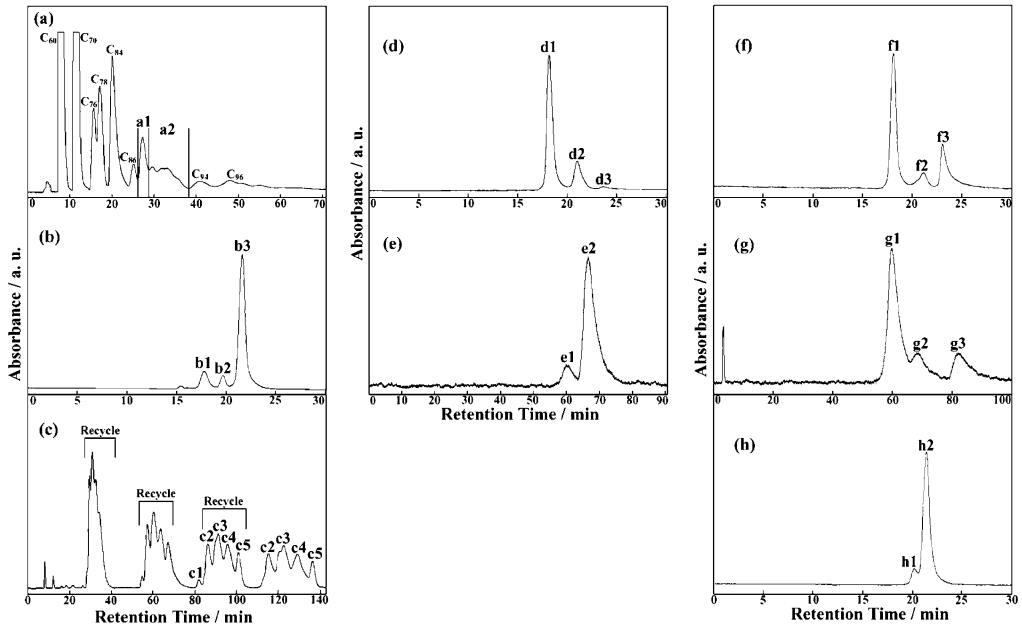

Figure 1. HPLC separation/isolation scheme of $(Y_2C_2)@C_{82}$(I, II) and $Y_2@C_{82}$(I, II): (a) first-stage HPLC chromatogram of the extract containing yttrium metallofullerenes on a 5PYE column; (b) second-stage HPLC chromatogram of fraction **a1** on a 5PYE column for $(Y_2C_2)@C_{82}$(I); (c) second-stage recycling HPLC chromatogram of fraction **a2** on a 5PYE column for $(Y_2C_2)@C_{82}$(II) and $Y_2@C_{82}$(I, II); (d, e) third- and fourth-stage HPLC chromatograms of $(Y_2C_2)@C_{82}$(II) on Buckyclutcher I and 5PBB columns, respectively; (f−h) third-, fourth-, and fifth-stage HPLC chromatograms of $Y_2@C_{82}$(I, II) on Buckyclutcher I, 5PBB, and Buckyclutcher I columns, respectively.

× 250 mm, Nacalai Tesque, 20 mL/min flow rate), and Buckyprep (20 mm diameter × 250 mm, Nacalai Tesque, 15 mL/min flow rate)] with toluene as eluent.

The purity of yttrium metallofullerenes was checked by both positive and negative laser desorption time-of-flight (LD-TOF) mass spectrometry as well as HPLC analyses. LD-TOF mass spectral data were obtained on a Shimadzu MALDI-IV mass spectrometer. UV−vis−NIR absorption spectra of yttrium metallofullerenes were measured in CS_2 solution by using a Jasco V-570 spectrophotometer.^{13}C NMR spectra of yttrium metallofullerenes in carbon disulfide solution were measured at a ^{13}C frequency of 150 MHz on a JEOL A-600 spectrometer. $Cr(acac)_3$ and benzene-d_6 were used as a relaxant and an internal rock, respectively. All ^{13}C NMR spectra were referenced to a CS_2 peak at 192.3 ppm.

Results and Discussion

Separation and Isolation of Yttrium Metallofullerenes. $(Y_2C_2)@C_{82}$(I, II, III) and $Y_2@C_{82}$(I, II, III) were isolated by the multistage high-performance liquid chromatography (HPLC) method.[1,32] Details of the separation of endohedral metallofullerenes have been described elsewhere.[1,22,28,29] Since the separation and isolation schemes of $(Y_2C_2)@C_{82}$(III) and $Y_2@C_{82}$(III) have been already reported,[22] we describe the separation schemes of $(Y_2C_2)@C_{82}$(I, II) and $Y_2@C_{82}$(I, II) in Figure 1. Figure 1a shows the first-stage HPLC chromatogram on the 5PYE column. Both $(Y_2C_2)@C_{82}$(I) and $Y@C_{82}$(I) exhibited almost the same retention times on the 5PYE column, whereas the retention times of $(Y_2C_2)@C_{82}$(II) and -(III) were significantly longer than that of $(Y_2C_2)@C_{82}$(I) under the same HPLC conditions.

Two fractions, **a1** and **a2**, were obtained on the first stage. Fraction **a1** contained $(Y_2C_2)@C_{82}$(I), $Y@C_{82}$(I), C_{84}, C_{86}, and C_{88}, whereas fraction **a2** consisted of $(Y_2C_2)@C_{82}$(II, III), $Y_2@C_{80}$, $Y@C_{82}$(I, II), $Y_2@C_{82}$(I, II, III), $Y_2@C_{86}$(I, II), C_{88}, C_{90}, and C_{92}. Figure 1b shows the second-stage HPLC chromatogram of fraction a1 on the Buckyclutcher I column. Fraction **a1** can be divided into three subfractions, **b1**−**b3**, at this stage. Fractions **b1**, **b2**, and **b3** contained C_{84}, C_{86} and C_{88}, and $(Y_2C_2)@C_{82}$(I) and $Y@C_{82}$(I), respectively. Finally, by recycling on the Buckyprep column, a small amount of other miscellaneous fullerenes was completely eliminated and the isolation of $(Y_2C_2)@C_{82}$(I) was achieved at this third stage (not shown in Figure 1).

Figure 1c shows the second-stage HPLC chromatogram for $(Y_2C_2)@C_{82}$(II, III) and $Y_2@C_{82}$(I, II, III). By recycling fraction **a2**, five subfractions from **c1** to **c5** were obtained. These five fractions contained the following yttrium-metallofullerenes together with empty higher fullerenes: fraction **c1** [C_{88}, $(Y_2C_2)@C_{82}$(I), and $Y@C_{82}$(I)] (tailing of fraction **a1**), fraction **c2** [C_{88}, $Y@C_{82}$(II), $Y_2@C_{82}$(I, II), and $Y_2@C_{86}$(I)], fraction **c3** [C_{90}, $Y_2@C_{82}$(I, II), and $(Y_2C_2)@C_{82}$(II, III)], fraction **c4** [C_{90}, $Y_2@C_{82}$(III), and $(Y_2C_2)@C_{82}$(III)], and fraction **c5** [C_{92}, $Y_2@C_{82}$(III), and $Y_2@C_{86}$(II)].

Figure 1 panels d and e show the third- and fourth-stage HPLC chromatograms of $(Y_2C_2)@C_{82}$(II) on the Buckyclutcher I and 5PBB columns, respectively. Fraction **c3** was divided into three subfractions, **d1**−**d3**, at this stage. These fractions contained yttrium-metallofullerenes and empty fullerenes: **d1** [C_{90}], **d2** [$(Y_2C_2)@C_{82}$(II) and $Y_2@C_{82}$(I, II)] and **d3** [$Y@C_{82}$(II)]. Fraction **d2** was divided into two subfractions, **e1** and **e2**, which contained $Y_2@C_{82}$(I, II) and $(Y_2C_2)@C_{82}$(II, III), respectively. Finally, by recycling on the Buckyprep column, a small amount of $(Y_2C_2)@C_{82}$(III) was completely eliminated and the isolation of $(Y_2C_2)@C_{82}$(II) was achieved at this fifth stage (not shown in Figure. 1).

Figure 1 panels f−h show the third-, fourth-, and fifth-stage HPLC chromatograms for $Y_2@C_{82}$(I, II) on Buckyclutcher I, 5PBB, and Buckyclutcher I columns, respectively. Fraction **c2** can be divided into three subfractions, from **f1** to **f3**, at this stage. These fractions contained the following yttrium-metallofullerenes and empty higher fullerenes: **f1** [C_{88}], **f2** [$Y_2@C_{82}$(I, II), $(Y_2C_2)@C_{82}$(II), and $Y_2@C_{86}$(I)] and **f3** [$Y@C_{82}$(II)]. Fraction **f2** was divided into three subfractions, from **g1** to **g3**,

at this stage. Fractions **g1**, **g2**, and **g3** contained, respectively, [$Y_2@C_{82}$(I, II)], [$(Y_2C_2)@C_{82}$(II) and $Y_2@C_{82}$ oxides], and [$Y_2@C_{86}$(I)]. Fraction **g1** was divided into two fractions, **h1** and **h2**, which contain $Y_2@C_{82}$(I) and $Y_2@C_{82}$(II), respectively. Finally, by recycling on the Buckyprep column, the isolation of $Y_2@C_{82}$(I, II) was achieved at this sixth stage (not shown in Figure 1). The isolation of each diyttrium metallofullerene was confirmed by both mass spectrometry and HPLC analyses.

The general tendency on retention times for fullerenes on 5PYE column is that elongated fullerenes have longer retention times than those of spherical fullerenes.[1,28,29] On the other hand, the retention times of fullerenes on 5PBB column strongly depend on the cage size (the number of carbon atoms on the cage) of fullerenes. For example, C_{80}(II)-D_{5d} isomer[33] is one of the most ellipsoidal fullerenes and has a much longer retention time than that of more spherical C_{80}(I)-D_2 isomer[34] on the 5PYE column (C_{80}(I), ca. 19 min, and C_{80}(II), ca. 26 min at 15 mL/min flow rate), whereas two isomers of C_{80} have essentially the same retention time on the 5PBB column (ca. 40 min at 20 mL/min flow rate).

The three isomers of $(Y_2C_2)@C_{82}$(I, II, III) have obviously different retention times on the 5PYE column, but they exhibit almost the same retention times on the 5PBB column (ca. 66−67 min at 20 mL/min flow rate). The retention time of $Y_2@C_{82}$-(III) on the 5PBB column (ca. 65 min at 20 mL/min flow rate) is essentially the same as those of $(Y_2C_2)@C_{82}$(I, II, III), suggesting that they possess the same fullerene cage, i.e., C_{82}. Clearly, this elution behavior of $(Y_2C_2)@C_{82}$(I, II, III) strongly suggests that these yttrium metallofullerenes have metal-carbide endohedral structures. Moreover, the retention times of $Y_2@C_{82}$-(I, II) are much shorter than those of $(Y_2C_2)@C_{82}$(I, II, III) and $Y_2@C_{82}$(III) on the 5PBB column (ca. 60 min at 20 mL/min flow rate) (cf. Figure 1e), suggesting that $Y_2@C_{82}$(I, II) might also have metal-carbide endohedral structures such as $(Y_2C_2)@C_{80}$.

UV−Vis−NIR Absorption Spectra of Yttrium Metallofullerenes. Figure 2 shows UV−vis−NIR absorption spectra of three isomers of $(Y_2C_2)@C_{82}$ in carbon disulfide solution. The absorption spectra of $(Y_2C_2)@C_{82}$(I, II, III) are different from each other. The spectrum of $(Y_2C_2)@C_{82}$(I) shows pronounced peaks at 629, 715, 791, 858, 1055, and 1204 nm. The onset of the spectrum is at ca. 1470 nm. $(Y_2C_2)@C_{82}$(II) shows broad absorption bands at 1466 and 1762 nm. The onset of $(Y_2C_2)@C_{82}$(II) lies down to 2200 nm, suggesting a small HOMO−LUMO gap. In fact, the solubility of $(Y_2C_2)@C_{82}$(II) in carbon disulfide is much lower than those of the other two isomers. The absorption feature of $(Y_2C_2)@C_{82}$(III) is less pronounced than those of isomers I and II. The characteristic absorption peaks are observed at 684 and 880 nm, and weak absorption bands are also seen at ca. 570, 790, and 1000 nm. The onset of the spectrum is at ca. 1100 nm, suggesting that the isomer has a large HOMO−LUMO energy gap as compared with isomers I and II. This is consistent with the observation that isomer III is the most abundant isomer among the three $(Y_2C_2)@C_{82}$ isomers.

During the course of the absorption measurements, we noticed that the absorption spectra of $(Y_2C_2)@C_{82}$(I, II, III) are similar to those of $Sc_2@C_{84}$(I, II, III),[15] respectively. Moreover, the absorption spectra of $Dy_2@C_{84}$(I, II, III)[29] are almost the same as those of $(Y_2C_2)@C_{82}$(I, II, III), respectively. In addition, the absorption spectrum of $Er_2@C_{84}$(I)[25] is also quite similar to that of $(Y_2C_2)@C_{82}$(I). It is generally known[1,32] that the UV−vis−NIR absorption spectra of fullerenes and metallofullerenes well reflect the cage size and symmetry. For example, the spectra of

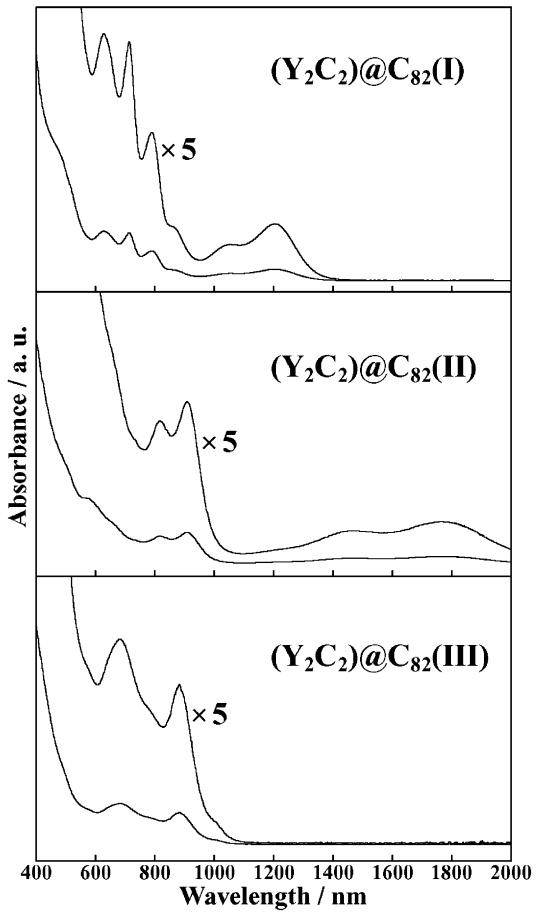

Figure 2. UV−Vis−NIR absorption spectra of $(Y_2C_2)@C_{82}$(I, II, III) in CS_2 solvent.

$M@C_{82}$ (M = Y, La, Ce, Pr, Gd etc.) show similar absorption features except for small band shifts.[35] The similarity of the absorption spectra among $(Y_2C_2)@C_{82}$(I, II, III), $Sc_2@C_{84}$(I, II, III),[15] $Dy_2@C_{84}$(I, II, III)[29] and $Eu_2@C_{84}$(I)[25] therefore strongly suggests that $Sc_2@C_{84}$(I, II, III) and $Dy_2@C_{84}$(I, II, III) also have carbide endohedral structures such as $(Sc_2C_2)@C_{82}$(I, II, III) and $(Dy_2C_2)@C_{82}$(I, II, III), respectively.

Figure 3 shows UV−vis−NIR absorption spectra of $Y_2@C_{82}$-(I, II, III) in carbon disulfide solution. These spectra are different from each other, suggesting that these metallofullerenes have different cages. The absorption spectrum of $Y_2@C_{82}$(I) exhibits a pronounced peak at 438 nm and broad absorption bands at 580, 650, 1379, 1642, and 1671 nm. The onset of the spectrum is at ca. 2100 nm, which is red-shifted with respect to other two isomers.

The spectrum of $Y_2@C_{82}$(II) is very rich in absorption features, showing absorption bands at 462, 642, 760, 958, 1142, and 1340 nm. The onset of the spectrum is at ca. 1600 nm. The absorption spectrum is similar to those of $Sc_2@C_{82}$(I)[28] and $Dy_2@C_{82}$(I),[29] suggesting that these metallofullerenes have the same cage structure.

The absorption spectrum of $Y_2@C_{82}$(III) shows only two characteristic absorption bands at 714 and 909 nm. The onset of the spectrum is at ca. 1100 nm, indicating that the metallofullerene has a large HOMO−LUMO energy gap like $(Y_2C_2)@C_{82}$(III). The absorption spectrum of $Y_2@C_{82}$(III) is almost identical with those of $M_2@C_{82}$(III) (M = Er, Tm).[12,27] The similarity of the spectra also suggests that all of these $M_2@C_{82}$(III) (M = Y, Er, Tm) metallofullerenes have the same C_{82} structure, presumably with an equal number of electron

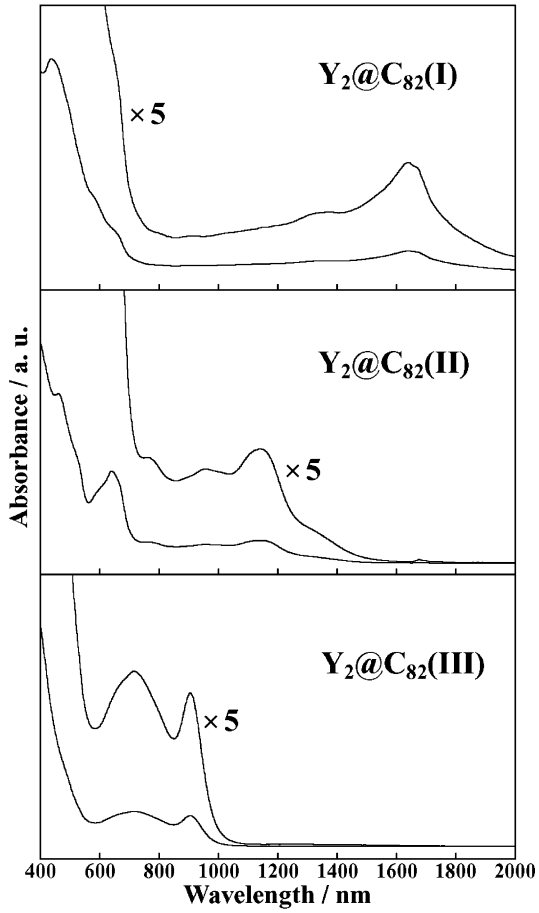

Figure 3. UV−Vis−NIR absorption spectra of $Y_2@C_{82}$(I, II, III) in CS_2 solvent.

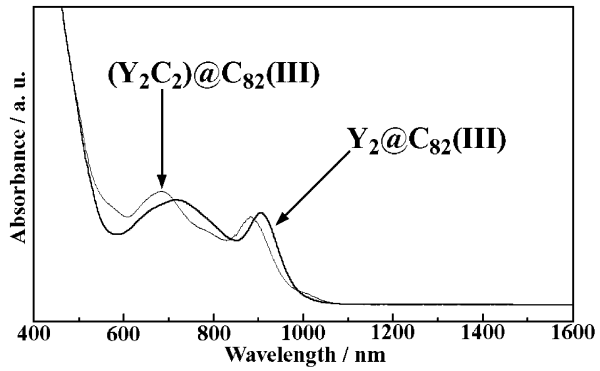

Figure 4. UV−Vis−NIR absorption spectra of $(Y_2C_2)@C_{82}$(III) and $Y_2@C_{82}$(III) in CS_2 solvent.

transfers from metal atoms to the carbon cage. Ding et al.[30] reported that the valency of Er in $Er_2@C_{82}$ is +3 and that the charge state on the C_{82} cage is expected to be −6. Furthermore, $Y_2@C_{82}$(III) and $Er_2@C_{82}$(III) exhibit quite similar retention times on the Buckyclutcher I column, which is known to sensitive to the amount of negative charge on the fullerene cage.[22,25] This suggests that $Y_2@C_{82}$(III) has the same isomer cage and charge state (−6) as those of $Er_2@C_{82}$(III).

$Y_2@C_{82}$(III) and $(Y_2C_2)@C_{82}$(III): Effect on Entrapment of a C_2 Radical. As shown in Figure 4, the absorption spectrum of $(Y_2C_2)@C_{82}$(III) is similar to that of $Y_2@C_{82}$(III), suggesting that they have the same C_{82} symmetry. However, slight peak shifts are observed on the corresponding absorption bands between $Y_2@C_{82}$(III) and $(Y_2C_2)@C_{82}$(III). Recently, Akasaka et al.[17,18] has reported that absorption bands of $La@C_{82}$ anion and cation are considerably shifted from that of neutral $La@C_{82}$. These shifts can be ascribed to the difference in the amount of the negative charge on the C_{82} cage. Similarly, the difference in the absorption bands between $(Y_2C_2)@C_{82}$(III) and $Y_2@C_{82}$(III) might be caused by the difference in the electron transfer from the metal atom to the C_{82} cage. Since the shift of the absorption bands is smaller than in the $La@C_{82}$ case, the entrapment of C_2 radical may induce only a slight reduction in the extent of electron transfer to the C_{82} cage.

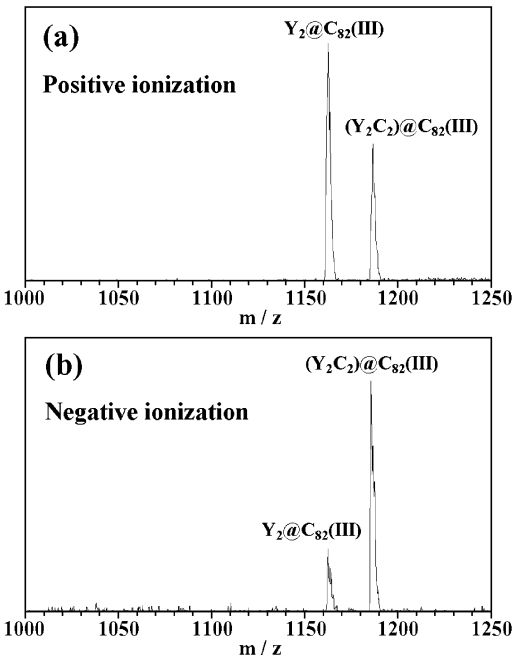

Figure 5. LD-TOF mass spectra of a mixed sample of $(Y_2C_2)@C_{82}$(III) and $Y_2@C_{82}$(III).

A characteristic absorption peak at 880 nm of $(Y_2C_2)@C_{82}$(III) is red-shifted to 909 nm for $Y_2@C_{82}$(III). This might indicate that LUMO level of $(Y_2C_2)@C_{82}$(III) slightly falls down from that of $Y_2@C_{82}$(III). The retention time of $(Y_2C_2)@C_{82}$(III) on Buckyclutcher I column is slightly shorter than that of $Y_2@C_{82}$(III).[22] This indicates that the extent of the electron transfer in $(Y_2C_2)@C_{82}$(III) should be slightly smaller than that occurring in $Y_2@C_{82}$(III). In fact, we already found that the electron transfer in $(Sc_2C_2)^{2+}@C_{84}^{2-}$ is much reduced from that of pure discandium fullerene $Sc_2^{4+}@C_{84}^{4-}$ as revealed by synchrotron X-ray analysis.[3,7]

The overall absorption spectral features of $(Y_2C_2)@C_{82}$(I, II, III) are similar to those of $M_2@C_{82}$(I, II, III) (M = Er and Tm),[12,27] respectively. The similarity on the absorption spectra between these metallofullerenes strongly suggests that they have the same C_{82} cages. The small shifts of absorption bands between these spectra are likely caused by the slight difference in the amounts of the electron transfer to the C_{82} cage as in the $(Y_2C_2)@C_{82}$(III) and $Y_2@C_{82}$(III) case described above.

Figure 5 shows typical LD-TOF mass spectra of a mixed sample of $(Y_2C_2)@C_{82}$(III) and $Y_2@C_{82}$(III). On the positive ionization mode spectrum, the signal due to $Y_2@C_{82}$(III) is much stronger than that of $(Y_2C_2)@C_{82}$(III). In contrast, the negative mode spectrum shows that $Y_2@C_{82}$(III) is detected as a weaker signal as compared with that of $(Y_2C_2)@C_{82}$(III). In fact, $Y_2@C_{82}$(III) is gradually oxidized to form $Y_2@C_{82}O$ species in toluene solvent at room temperature, whereas $(Y_2C_2)@C_{82}$(III) is totally stable in the same condition. Such a tendency to oxidation of $Y_2@C_{82}$(III) is consistent with the observation that the metallofullerene likes to form cationic species from LD-TOF mass spectrometry.

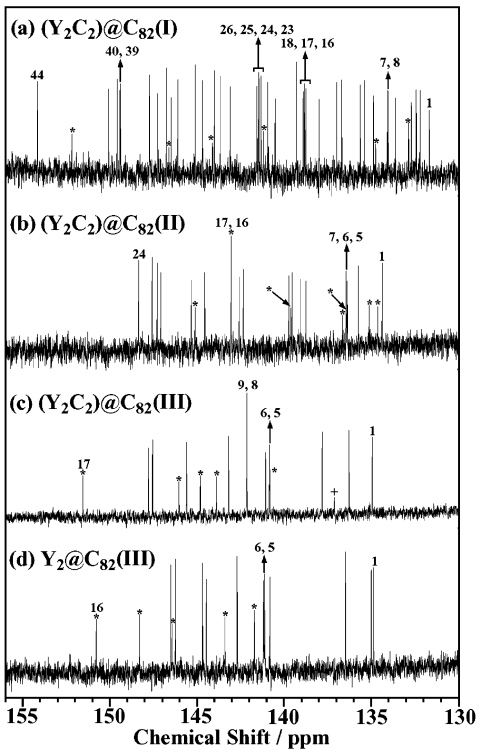

Figure 6. ^{13}C NMR spectra of $(Y_2C_2)@C_{82}$(I, II, III) and $Y_2@C_{82}$(III) in CS_2 solvent at room temperature. The marked signals have (*) half and (+) $^1/_6$ intensity, respectively.

Structural Analyses by ^{13}C NMR Measurements. ^{13}C NMR spectra of $(Y_2C_2)@C_{82}$(I, II, III) and $Y_2@C_{82}$(III) in carbon disulfide at room temperature are shown in Figure 6. The ^{13}C NMR spectra of three isomers of $(Y_2C_2)@C_{82}$ consist of the following number of signals and relative intensity: isomer I [38 full-intensity and six half-intensity signals], isomer II [17 full-intensity and six half-intensity signals], and isomer III [11 full-intensity, five half-intensity and one $^1/_6$ intensity signal] (cf. Table 1). From these NMR signal intensity/pattern, isomers I, II, and III of $(Y_2C_2)@C_{82}$ have the molecular symmetry C_s, C_{2v}, and C_{3v}, respectively. However, none of the isolated pentagon rule (IPR)[36] isomers of C_{84} can satisfy the present ^{13}C NMR spectral patterns of $(Y_2C_2)@C_{82}$(I, II, III). Instead, the observed ^{13}C NMR patterns satisfy the ^{13}C NMR patterns of three isomers of C_{82} (Table 2), indicating that $(Y_2C_2)@C_{82}$(I, II, III) are metal-carbide endohedral fullerenes[7] in which a Y_2C_2 cluster is encapsulated by the C_{82} cage. The first metal-carbide endohedral metallofullerene was synthesized and structurally characterized in our laboratory for $(Sc_2C_2)@C_{84}$.[7]

The cages of isomers II and III of $(Y_2C_2)@C_{82}$ can safely be assigned to C_{82}-C_{2v}(9) and C_{82}-C_{3v}(8), respectively. Isomer I may have a symmetry reduction by the presence of an Y_2C_2 endohedral species. Three C_s (2, 4, and 6) cages of C_{82} can satisfy the observed NMR pattern of $(Y_2C_2)@C_{82}$(I). If an Y_2C_2 cluster is located on the symmetry plane of C_{82}-C_{3v}(8) cage and is displaced from the C_3 axis, the entire molecular symmetry becomes C_s symmetry (symmetry reduction) and the C_{3v}(8) cage also satisfies the observed signal/intensity pattern. Therefore, the four cages, three C_s and one C_{3v}(8) isomer, can be the candidates for the C_{82} cage of $(Y_2C_2)@C_{82}$(I).

The absorption spectrum of $(Y_2C_2)@C_{82}$(I) is very similar to that of $Er_2@C_{82}$(I),[12,25,27] and HPLC retention times of $(Y_2C_2)@C_{82}$(I) and $Er_2@C_{82}$(I) on the Buckyclutcher I column are almost the same.[25] The cage structure of $Er_2@C_{82}$(I) is C_{82}-C_s(6) as obtained by an X-ray diffraction experiment.[12] Thus, together with the NMR result, $(Y_2C_2)@C_{82}$(I) also possesses a C_{82}-C_s(6) cage. Figure 7 presents probable molecular structures of $(Y_2C_2)@C_{82}$(I, II, III) consistent with the ^{13}C NMR results.

$(Y_2C_2)@C_{82}$(II) is a metal-carbide endohedral metallofullerene in which a Y_2C_2 carbide cluster is encapsulated in the C_{82}-C_{2v}(9) cage. This is the first experimental confirmation that a major dimetallofullerene also has the C_{82}-C_{2v}(9) cage, which has been well-known as the cage for the most abundant $M@C_{82}$

TABLE 1: ^{13}C NMR Chemical Shifts[a] for $(Y_2C_2)@C_{82}$(I, II, III) and $Y_2@C_{82}$(III)

$(Y_2C_2)@C_{82}$(I) C_s	$(Y_2C_2)@C_{82}$(II) C_{2v}(9)	$(Y_2C_2)@C_{82}$(III) C_{3v}(8)	$Y_2@C_{82}$(III) C_{3v}(8)
131.64	134.33	134.95	134.84
132.18	134.59*	136.28	134.98
132.39	135.08*	137.12+	136.46
132.68	135.70	137.82	140.80
132.84*	136.34	140.83*	141.10
133.60	136.39*	140.85	141.17
133.99	136.40	141.06	141.69*
134.05	136.60*	142.13	142.68
134.73*	138.70	142.14	143.39*
134.86	139.01	143.19	144.46
135.40	139.51	143.89*	144.68
135.62	139.57*	144.81*	146.23
136.68	139.69	145.60	146.39*
136.97	142.31	146.05*	146.49
137.98	142.54	147.56	148.29*
138.75	143.01*	147.80	150.78*
138.83	143.01	151.57*	
138.91	144.53		
139.28	145.08		
140.52	145.29		
140.95	147.05		
141.18*	147.26		
141.33	147.55		
141.45	148.32		
141.47			
141.56			
143.11			
143.68			
144.02			
144.13*			
144.70			
145.13			
146.12			
146.50			
146.63*			
146.78			
147.28			
147.76			
149.43			
149.45			
149.62			
150.11			
152.22*			
154.20			

[a] Chemical shifts are given in parts per million.

TABLE 2: Nine Isomers of C_{82} Fullerenes That Satisfy the Isolated Pentagon Rule

isomer	point group	^{13}C NMR pattern[a]
1	C_2	41(2)
2	C_s	38(2), 6(1)
3	C_2	41(2)
4	C_s	38(2), 6(1)
5	C_2	41(2)
6	C_s	38(2), 6(1)
7	C_{3v}	12(6), 3(3), 1(1)
8	C_{3v}	11(6), 5(3), 1(1)
9	C_{2v}	17(4), 7(2)

[a] Number of signals (number of equivalent carbon atoms).

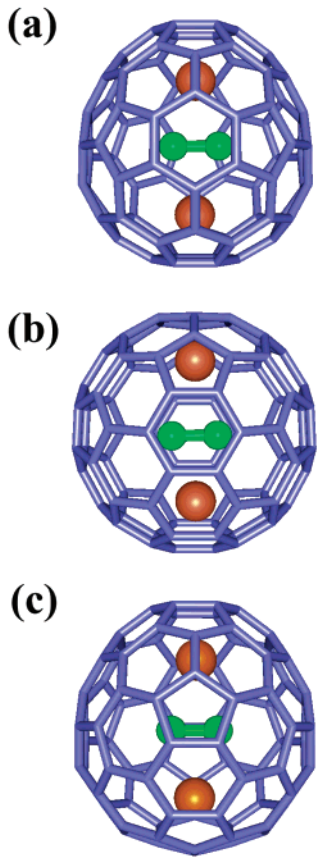

Figure 7. Molecular structures of $(Y_2C_2)@C_{82}$(I, II, III) consistent with the ^{13}C NMR results. The C_{82} cage, yttrium atoms, and C_2 species are colored blue, brown, and green, respectively.

(M = Y, Sc, La, Ce, Gd, etc.) type monometallofullerene.[1,2,4,6,17,18,20,25,29,32,35] The C_{82}-C_{2v}(9) cage is a "magic fullerene cage" not only for the monometallofullerenes but also for dimetallofullerenes such as $(Y_2C_2)@C_{82}$(II) and $Y@C_{82}$.

$(Y_2C_2)@C_{82}$(III) is a metal-carbide endohedral metallofullerene. Details of the analysis of the ^{13}C NMR spectrum have already been reported.[22]

Attempts to detect ^{13}C NMR signals of the encapsulated C_2 species of the $(Y_2C_2)@C_{82}$(I, II, III) have not been successful so far. No salient peaks due to C_2 in $(Y_2C_2)@C_{82}$(III) have been observed at temperatures down to 238 K. In contrast, a weak ^{13}C NMR signal due to C_2 species of Sc_2C_2 in $(Sc_2C_2)@C_{84}$ was observed.[7] The inability to observe NMR signals from the encaged C_2 might be explained within the framework of the spin−rotation interaction.[16,22] For $(Y_2C_2)@C_{82}$(III), we have already reported that a diamondlike Y_2C_2 cluster should rotate rapidly around the C_3 axis of the spherical C_{82}-C_{3v}(8) cage in order to maintain the entire molecular symmetry C_{3v}.[22] The rotation of C_2 in the cage is still too rapid for signals to be detected, at least at 238 K.

Structures of $Y_2@C_{82}$ and $(Y_2C_2)@C_{82}$: A Clue for Growth Mechanisms on Metallofullerenes. The ^{13}C NMR spectrum of $Y_2@C_{82}$(III) shows 11 full-intensity and five half-intensity signals (Figure 6d). The NMR features are similar to those of $(Y_2C_2)@C_{82}$(III) (Figure 6c): (i) three distinct full-intensity signals are observed in the downfield region at 134.84, 134.98, and 136.46 ppm; (ii) a characteristic half-intensity signal is observed higher than 150 ppm; and (iii) the entire chemical shift range of the signals is very similar. Moreover, the absorption spectrum of $Y_2@C_{82}$(III) is similar to that of $(Y_2C_2)@C_{82}$(III) (cf. Figure 4). These similarities strongly suggest that

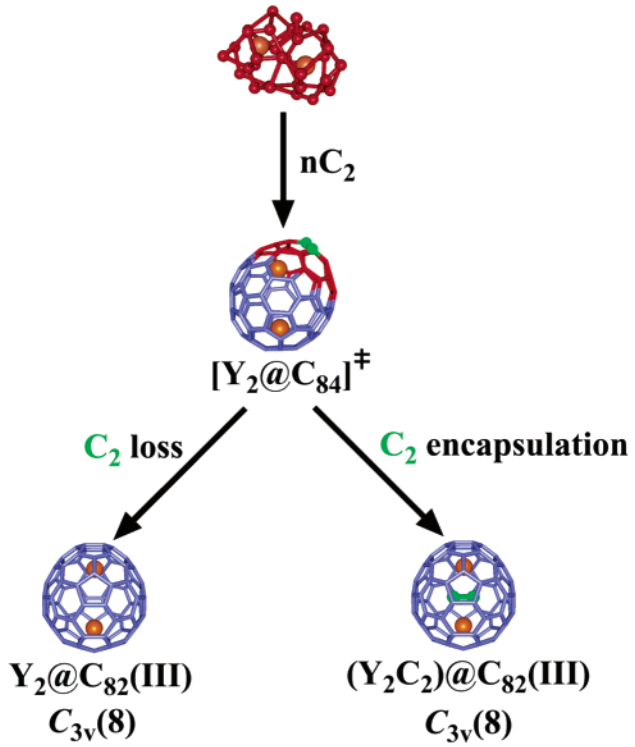

Figure 8. Proposed growth mechanism for diyttrium metallofullerenes $Y_2@C_{82}$(III) and $(Y_2C_2)@C_{82}$(III).

$Y_2@C_{82}$(III) and $(Y_2C_2)@C_{82}$(III) have the same C_{82} cage [i.e., C_{82}-C_{3v}(8)]. The only structural difference between $(Y_2C_2)@C_{82}$(III) and $Y_2@C_{82}$(III) is the presence and absence of C_2 species in the cage, respectively. Furthermore, the similarity of the absorption spectra between $M_2@C_{82}$(I, II, III) (M = Er, Tm)[12,27] and $(Y_2C_2)@C_{82}$(I, II, III) strongly suggests that each of these corresponding isomers has the same C_{82} cage.

The existence of $(Y_2C_2)@C_{82}$(III) and $Y_2@C_{82}$(III) with exactly the same cage structure can strongly support an idea that $Y_2@C_{84}$ is much less stable than $(Y_2C_2)@C_{82}$(III) and $Y_2@C_{82}$(III). In fact, we found that the abundance of the pure diyttrium C_{84} metallofullerene $Y_2@C_{84}$ is substantially lower than that of C_{82}-based diyttrium fullerenes such as $Y_2@C_{82}$ and $(Y_2C_2)@C_{82}$.[37] Presently, we think that at the final stage of the growth $Y_2@C_{84}$ preferentially evaporates C_2 (the so-called C_2-loss process) either outward or inward of the cage to stabilize the fullerenes, which leads to pure $Y_2@C_{82}$ and carbide $(Y_2C_2)@C_{82}$ metallofullerenes, respectively (Figure 8). Such evaporating/cooling processes of metallofullerenes via encapsulation of C_2 species inside the cages have actually been observed in various Sc-metallofullerenes such as $Sc_2@C_{84}$ and $Sc_3@C_{82}$ by a gas-phase ion chromatographic experiment.[38]

Conclusion

Diyttrium metallofullerenes $(Y_2C_2)@C_{82}$(I, II, III) and $Y_2@C_{82}$(I, II, III) were synthesized, isolated, and characterized by UV−vis−NIR absorption spectroscopy. The ^{13}C NMR spectra of $(Y_2C_2)@C_{82}$(I, II, III) showed that their symmetries were C_s, C_{2v}(no. 9), and C_{3v}(no. 8), respectively. $(Y_2C_2)@C_{82}$(II) has an identical cage with the most abundant $M@C_{82}$(I)-type monometallofullerenes. The most abundant diyttrium metallofullerenes were found to be metal-carbide endohedral fullerenes $(Y_2C_2)@C_{82}$(I, II, III).

The ^{13}C NMR spectrum of $Y_2@C_{82}$(III) revealed that the cage is exactly the same as that of $(Y_2C_2)@C_{82}$(III), i.e. C_{82}-C_{3v}(8). The only structural difference between $Y_2@C_{82}$(III) and

$(Y_2C_2)@C_{82}$(III) is the presence and absence of C_2 species in the cage, respectively. We propose that, at the final stage of growth, highly excited $Y_2@C_{84}$ preferentially evaporates C_2 (the so-called C_2-loss process) either outward or inward of the cage to stabilize the fullerenes, which leads to pure $Y_2@C_{82}$ and carbide $(Y_2C_2)@C_{82}$ metallofullerenes, respectively.

References and Notes

(1) Shinohara, H. *Rep. Prog. Phys.* **2000**, *63*, 843.

(2) Takata, M.; Umeda, B.; Nishibori, E.; Sakata, M.; Saito, Y.; Ohno, M.; Shinohara, H. *Nature* **1995**, *377*, 46.

(3) Takata, M.; Nishibori, E.; Umeda, B.; Sakata, M.; Yamamoto, E.; Shinohara, H. *Phys. Rev. Lett.* **1997**, *78*, 3330.

(4) Nishibori, E.; Takata, M.; Sakata, M.; Inakuma, M.; Shinohara, H. *Chem. Phys. Lett.* **1998**, *298*, 79.

(5) Takata, M.; Nishibori, E.; Sakata, M.; Inakuma, M.; Yamamoto, E.; Shinohara, H. *Phys. Rev. Lett.* **1999**, *83*, 2214.

(6) Nishibori, E.; Takata, M.; Sakata, M.; Tanaka, H.; Hasegawa, M.; Shinohara, H. *Chem. Phys. Lett.* **2000**, *330*, 497.

(7) Wang, C.-R.; Kai, T.; Tomiyama, T.; Yoshida, T.; Kobayashi. Y.; Nishibori, E.; Takata, M.; Sakata, M.; Shinohara, H. *Angew. Chem., Int. Ed.* **2001**, *40*, 397.

(8) Wang, C.-R.; Kai, T.: Tomiyama, T.; Yoshida, T.; Kobayashi, Y.; Nishibori, E.; Takata, M.; Sakata, M.; Shinohara, H. *Nature* **2000**, *408*, 426.

(9) Nishibori, E.; Takata, M.; Sakata, M.; Taninaka, A.; Shinohara, H. *Angew. Chem., Int. Ed.* **2001**, *40*, 2998.

(10) Stevenson, S.; Rice, G.; Glass, T.; Harich, K.; Cromer, F.; Jordan, M. R.; Craft, J.; Hadju, E.; Bible, R.; Olmstead, M. M.; Maitra, K.; Fisher, A. J.; Balch, A. L.; Dorn, H. C. *Nature* **1999**, *401*, 55.

(11) Olmstead, M. M.; de Bettencourt-Dias, A.; Duchamp, J. C.; Stevenson, S.; Dorn, H. C.; Balch, A. L. *Angew. Chem., Int. Ed.* **2001**, *40*, 1223.

(12) Olmstead, M. M.; de Bettencourt-Dias, A.; Stevenson, S.; Dorn, H. C.; Balch, A. L. *J. Am. Chem. Soc.* **2002**, *124*, 4172.

(13) Olmstead, M. M.; Lee, H. M.; Duchamp, J. C.; Stevenson, S.; Marciu, D.; Dorn, H. C.; Balch, A. L. *Angew. Chem., Int. Ed.* **2003**, *42*, 900.

(14) Yamamoto, E.; Tansho, M.; Tomiyama, T.; Shinohara, H.; Kawahara, H.; Kobayashi, Y. *J. Am. Chem. Soc.* **1996**, *118*, 2293.

(15) Inakuma, M.; Yamamoto, E.; Kai, T.; Wang, C.-R.; Tomiyama, T.; Shinohara, H.; Dennis, T. J. D.; Hulman, M.; Krause, M.; Kuzmany, H. *J. Phys. Chem. B* **2000**, *104*, 5072.

(16) Akasaka, T.; Nagase, S.; Kobayashi, K.; Wälchli, M.; Yamamoto, K.; Funasaka, H.; Kako, M.; Hoshino, T.; Erata, T. *Angew. Chem., Int. Ed. Engl.* **1997**, *36*, 1643.

(17) Akasaka, T.; Wakahara, T.; Nagase, S.; Kobayashi, K.; Wälchli, M.; Yamamoto, K.; Kondo, M.; Shirakura, S.; Okubo, S.; Maeda, Y.; Kato, T.; Kako, M.; Nakadaira, Y.; Nagahata, R.; Gao, X.; Van Caemelbecke, E.; Kadish, K. M. *J. Am. Chem. Soc.* **2000**, *122*, 9316.

(18) Akasaka, T.; Wakahara, T.; Nagase, S.; Kobayashi, K.; Wälchli, M.; Yamamoto, K.; Kondo, M.; Shirakura, S.; Maeda, Y.; Kato, T.; Kako, M.; Nakadaira, Y.; Gao, X.; Van Caemelbecke, E.; Kadish, K. M. *J. Phys. Chem. B* **2001**, *105*, 2971.

(19) Wang, C.-R.; Georgi, P.; Dunsch, L.; Kai, T.; Tomiyama, T.; Shinohara, H. *Curr. Appl. Phys.* **2002**, *2*, 141.

(20) Kodama, T.; Ozawa, N.; Miyake, Y.; Sakaguchi, K.; Nishikawa, H.; Ikemoto, I.; Kikuchi, K.; Achiba, Y. *J. Am. Chem. Soc.* **2002**, *124*, 1452.

(21) Kodama, T.; Fujii, R.; Miyake, Y.; Sakaguchi, K.; Nishikawa, H.; Ikemoto, I.; Kikuchi, K.; Achiba, Y. *Chem. Phys. Lett.* **2003**, *377*, 197.

(22) Inoue, T.; Tomiyama, T.; Sugai, T.; Shinohara, H. *Chem. Phys. Lett.* **2003**, *382*, 226.

(23) Shinohara, H.; Sato, H.; Saito, Y.; Ohkohchi, M.; Ando, Y. *J. Phys. Chem.* **1992**, *96*, 3571.

(24) Weaver, J. H.; Chai, Y.; Kroll, G. H.; Jin, C.; Ohno, T. R.; Haufler, R. E.; Guo, T.; Alford, J. M.; Conceicao, J.; Chibante, L. P. F.; Jain, A.; Palmer, G.; Smalley, R. E. *Chem. Phys. Lett.* **1992**, *190*, 460.

(25) Tagmatarchis, N.; Aslanis, E.; Shinohara, H.; Prassides, K. *J. Phys. Chem. B* **2000**, *104*, 11010.

(26) Heflin, J. R.; Marciu, D.; Figura, C.; Wang, S.; Burbank, P.; Stevenson, S.; Dorn, H. C. *Appl. Phys. Lett.* **1998**, *72*, 2788.

(27) Kikuchi, K.; Akiyama, K.; Sakaguchi, K.; Kodama, T.; Nishikawa, H.; Ikemoto, I.; Ishigaki, T.; Achiba, Y.; Sueki, K.; Nakahara, H. *Chem. Phys. Lett.* **2000**, *319*, 472.

(28) Wang, C.-R.; Inakuma, M.; Shinohara, H. *Chem. Phys. Lett.* **1999**, *300*, 379.

(29) Tagmatarchis, N.; Shinohara, H. *Chem. Mater.* **2000**, *12*, 3222.

(30) Ding, X.; Alford, J. M.; Wright, J. C. *Chem. Phys. Lett.* **2000**, *319*, 472.

(31) Macfarlane, R. M.; Wittmann, G.; van Loosdrecht, P. H. M.; de Vries, M.; Bethune, D. S.; Stevenson, S.; Dorn, H. C. *Phys. Rev. Lett.* **1997**, *79*, 1397.

(32) Xu, Z.; Nakane, T.; Shinohara, H. *J. Am. Chem. Soc.* **1996**, *118*, 11309.

(33) Wang, C.-R.; Sugai, T.; Kai, T.; Tomiyama, T.; Shinohara, H. *Chem. Commun.* **2000**, 557.

(34) Hennrich, F. H.; Michel, R. H.; Fischer, A.; Richard-Schneider, S.; Grib, S.; Kappes, M. M.; Fuchs, D.; Bürk, M.; Kobayashi, K.; Nagase, S. *Angew. Chem., Int. Ed. Engl.* **1996**, *35*, 1732.

(35) Akiyama, K.; Sueki, K.; Kodama, T.; Kikuchi, K.; Ikemoto, I.; Katada, M.; Nakahara, H. *J. Phys. Chem. A* **2000**, *104*, 7224.

(36) Fowler, P. W.; Manolopoulos, D. E. *An Atlas of Fullerenes*; Oxford University Press: Oxford, U.K., 1995.

(37) Inoue, T., Tomiyama, T., Sugai, T., Okazaki, T., Nishibori, E., Takata, M., Sakata, M., and Shinohara, H., unpublished results.

(38) Sugai, T.; Inakuma, M.; Hudgins, R.; Dugourd, P.; Fye, J. L.; Jarrold, M. F.; Shinohara, H. *J. Am. Chem. Soc.* **2001**, *123*, 6427.